ACTA NEUROBIOLOGIAE EXPERIMENTALIS

Research Paper Acta Neurobiol Exp 2014, 74: 197–210

Early increase of cannabinoid receptor density after experimental traumatic brain injury in the newborn piglet

Cornelius K. Donat[1]*, Felix Fischer[1], Bernd Walter[2], Winnie Deuther-Conrad[1], Michael Brodhun[3], Reinhard Bauer[4], and Peter Brust[1]

[1]Department of Neuroradiopharmaceuticals, Institute of Radiopharmaceutical Cancer Research, Research Site Leipzig, Helmholtz-Zentrum Dresden-Rossendorf, Leipzig, Germany, *Email: cdonat@nru.dk; [2]Heinrich Braun Hospital, Zwickau, Germany; [3]Department of Pathology, Helios-Klinikum Erfurt, Erfurt, Germany; [4]Institute of Molecular Cell Biology and Center for Sepsis Control and Care (CSCC), Jena University Hospital, Jena, Germany

Paediatric traumatic brain injury (TBI) is a leading cause of death and disability. Previous studies showed neuroprotection after TBI by (endo)cannabinoid mechanisms, suggesting involvement of cannabinoid receptors (CBR). We therefore determined CBR densities and expression of the translocator protein 18 kDA (TSPO) in newborn piglets after experimental TBI. Newborn female piglets were subjected to sham operation (n=6) or fluid-percussion (FP) injury (n=7) under controlled physiological conditions. After six hours, brains were frozen, sagittally cut and incubated with radioligands for CBR ([^{3}HCP-55,940, [^{3}H]SR141716A) and TSPO ([^{3}H]PK11195), an indicator of gliosis/brain injury. Early after injury, FP-TBI elicited a significant ICP increase at a temporary reduced cerebral perfusion pressure; however, CBF and $CMRO_2$ remained within physiological range. At 6 hours post injury, we found a statistically significant increase in binding of the non-selective agonist [^{3}H]CP-55,940 in 15 of the 24 investigated brain regions of injured animals. By contrast, no significant changes in binding of the CB1R-selective antagonist [^{3}H]SR141716A were observed. A non-significant trend towards increased binding of [^{3}H]PK11195 was observed, suggesting an incipient microglial activation.We therefore conclude that in this model and time span after injury, the increase in [^{3}H]CP-55,940 binding reflects changes in CB2R density, while CB1R density is not affected. The results may provide explanation for the neuroprotective properties of cannabinoid ligands and future therapeutic strategies of TBI.

Key words:traumatic brain injury, autoradiography, cannabinoid receptors, neuroprotection

ABBREVIATIONS:

2-AG – 2-arachidonylglycerol
CBR – cannabinoid receptor
CB1R – cannabinoid receptor 1
CB2R – cannabinoid receptor 2
CBF – cerebral blood flow
CMS – coloured microsphere
eCB – endocannabinoids
FP – fluid percussion
TBI – traumatic brain injury
TSPO – translocator protein 18 kDA

Correspondence should be addressed to C.K. Donat
Email: cdonat@nru.dk

Received 22 November 2013, accepted 27 March 2014

INTRODUCTION

Traumatic brain injury (TBI) is a disease of worldwide impact, with different pathological mechanisms sharing aspects with other neurological diseases. In paediatrics, TBI is still the main reason of death and long lasting disabilities (Keenan and Bratton 2006). Because paediatric and adult TBI differ in biomechanics and molecular pathways (Bauer and Fritz 2004, Giza et al. 2007), the identification of pathophysiologic processes in paediatric TBI requires additional research effort (Jankowitz and Adelson 2006, Kochanek 2006). Early publications suggested that the higher plasticity of the immature brain would allow a better recovery after traumatic insults to the brain (Kennard 1942). However, most recent studies show that infants

are much more affected by the developmental outcomes after TBI than adults (Anderson et al. 2005, Barlow et al. 2005). Systematic reviews revealed that up to 50% of children with TBI later suffer from TBI-associated neurological impairments (Li and Liu 2013), resulting in serious socioeconomic consequences (Taylor et al. 2008, Anderson et al. 2009).

TBI is now seen as a complex, multifactorial disease process with interconnected pathogenetic pathways, e.g. excitotoxicity and cerebral ischemia (Masel and DeWitt 2010), following the initial biomechanical impact. Molecular changes after TBI include, for example, the excessive release of glutamate (Luo et al. 2011), influx of calcium (Weber 2004), followed by free radical generation, oxidative stress and neuroinflammation, causing necrosis and apoptosis (Bayir et al. 2006, Cederberg and Siesjo 2010).

Major neurotransmitter systems (e.g. glutamatergic, cholinergic, monaminergic) were investigated in TBI to understand the secondary injury effects with the intention to develop receptor-specific treatment options. However, while some trials are still ongoing, many failed (Tolias and Bullock 2004, McConeghy et al. 2012). Compared to stroke, the successful translation of these novel treatment attempts is rather limited (Li et al. 2014). Recently, modulation of neurotransmission was suggested to be more promising for directed interventions (Miller and Devi 2011). The endocannabinoid system, consisting of the endogenous cannabinoid ligands (eCBs) anandamide and 2-arachidonylglycerol (2-AG), cannabinoid receptors 1 and 2 (CBR, CB1R/CB2R) and associated enzymes, transporters and agonists, is exerting many neuromodulatory effects and may provide treatment options (Sarne et al. 2011, Shohami et al. 2011). Unlike 'classical' neurotransmitters, the eCBs are not stored in presynaptic vesicles, but are synthesized 'on demand' e.g. due to increased intracellular calcium concentration. The eCB system has been shown to be activated in response to pathogenic events, such as excitotoxicity, neuroinflammation and brain injury, suggesting that the eCB are part of the brain's compensatory or repair mechanisms (Bahr et al. 2006). The eCB levels are increased after TBI and administration of eCBs or CBR agonists in experimental injury reduced oedema and the neuroinflammatory response, while recovery was increased (Panikashvili et al. 2001, Shohami et al. 2011). However, it is still not clear whether these improvements are related to CBR, because the effects of TBI on regional CBR expression in the (immature) brain have not yet been determined. Therefore, we investigated CBR densities and the expression of the translocator protein 18 kDA (TSPO) with *in vitro* autoradiography after fluid percussion (FP) injury in newborn piglets. We postulate that the acute biomechanical and/or secondary effects of severe TBI on the brain may alter regional CBR expression in a large, gyrencephalic model of diffuse juvenile TBI.

METHODS

The experimental protocols were approved by the local ethics committee and are in compliance with national and EC (EC Directive 86/609/EEC) regulations for animal research. The chemicals were purchased from Sigma-Aldrich, Germany if not otherwise stated.

Surgical preparations, monitoring procedures and fluid-percussion (FP) administration

Thirteen crossbred female piglets were used (Deutsches Edelschwein, 7.7±1.2 days old, 3.1±0.3 kg body weight). Animals were initially anaesthetized with 2.5% isoflurane in nitrous oxide and oxygen and maintained throughout the surgical procedure with 1.3% isoflurane. Body temperature was maintained at 38.3±0.2°C with infrared lamps, controlled by a rectal thermal probe. Animals were paralysed with pancuronium bromide (0.2 mg/kg/h) and mechanically ventilated (Servo Ventilator 900C, Siemens-Elema, Solna, Sweden). The ventilator was set with a positive inspiratory pressure of 15–20 mbar and a positive end-expiratory pressure of 2–4 mbar. Respiratory rate and inspired oxygen fraction were titrated to maintain a $PaCO_2$ of 35–40 mm Hg and PaO_2 of 100–130 mm Hg. Polyurethane catheters (1.2 mm outer diamenter) were inserted in both saphenous arteries and advanced to the abdominal aorta for blood pressure/blood gas monitoring and withdrawal of arterial blood samples, including the reference samples for the colored microsphere (CMS) technique. A left thoracotomy was then performed through the third intercostal space and a catheter was inserted into the left atrium for injection of CMS to determine cerebral blood flow (CBF). A further catheter (inner diameter 0.3 mm) was inserted into the superior sagittal sinus through a midline burr hole (diameter 3 mm, 4 mm caudal to bregma) and

advanced to the confluence of the sinuses in order to obtain brain venous blood samples. All animals received a craniotomy, centered between lambda and bregma over the right parietal cortex, with intact dura, in order to fix the fluid percussion adapter (with a 12-mm bore of tube). A further hole was drilled into the left parietal bone and a fiberoptic catheter was implanted into the subcortical white matter for intracranial pressure (ICP) measurements (Camino Laboratories, San Diego, USA). The burr holes were sealed with bone wax and covered with dental acrylic resin in order to fix probes and the fluid percussion adapter in place thoughout the experiment.

The regional CBF was measured by means of the reference sample colour-labelled microsphere (DyeTrak®, Triton Technology, San Diego, USA) technique, which represents a valid alternative to the radioactively labelled microsphere method for organ blood flow measurement in newborn piglets (Walter et al. 1997). Application in piglets and methodical considerations have been presented and discussed in detail elsewhere (Walter et al. 1997). Briefly, in random sequence between 900 thousand and 1.2 million colored polystyrene microspheres were injected into the left atrium. The injection line was then flushed with 2 mL of saline. A blood sample was withdrawn from the abdominal aorta as the reference sample (Makowski et al. 1968), beginning 15 s before the microsphere injection and continuing for 2 min at a rate of 1.50 mL/min (syringe pump SP210iw, World Precision Instruments Inc., Sarasota, USA). At the end of each experiment, the brains were quickly removed; dissected midline in the sagittal plane and the right part (opposite to fluid percussion trauma administration) was sectioned in the desired brain regions. For digestion, reference blood samples and tissue samples of 0.5–2.5 g were covered with an appropriate volume (approximately 3 mL/g) of digestive solution (4 N KOH with 4% Tween 80 in deionized water). All tissue and blood samples were digested for a minimum of 4 h at 60°C. In order to isolate the microspheres, each tissue sample was digested and then filtered under vacuum suction through an 8 μm pore polyester-membrane filter. Colored microspheres were quantified by their dye content. The dye was recovered from the microspheres by adding dimethyl-formamide. The photometric absorption of each dye solution was measured by a diode-array UV/visible spectrophotometer (model 7500, Beckman Instruments, Fullerton, USA). Calculations were performed using the MISS® software (Triton Technology). The number of microspheres was calculated using the specific absorbance value of the different dyes. All reference and tissue samples contained >400 microspheres.

The heart rate, the arterial blood pressure, the arterial and brain venous pH, PCO_2, and PO_2, and O_2 content, were measured immediately before the microsphere injection. The blood pH, PCO_2, and PO_2 were determined with a blood gas analyzer (model ABL50, Radiometer, Copenhagen, Denmark). The O_2 content was measured using a hemoximeter (model OSM3, Radiometer, Copenhagen, Denmark), and corrected to the body temperature of the animal at the time of sampling. The absolute flows to the tissues measured by the colored microspheres were calculated by the formula:

$$flow_{tissue} = \text{number of microspheres}_{tissue} \times (flow_{reference} / \text{number of microspheres}_{reference}).$$

The flows are expressed in milliliters per min per 100g tissue by normalizing for tissue weight. The $CMRO_2$ was obtained by multiplying the blood flow to the forebrain by the cerebral arteriovenous O_2 content difference, where the blood flow to the forebrain includes all regions drained by the sagittal sinus [cerebral cortex, cerebral white matter, some deep gray structures: basal ganglia, thalamus, and hippocampus (Coyle et al. 1993)].

Fluid percussion (FP) administration and experimental protocol

Eleven randomly chosen piglets were subjected to FP injury. A self-made device designed according to Sullivan and coworkers (1976) was used. The fluid percussion adapter was attached to a transduced housing and connected to the fluid percussion device. The device consisted of a Plexiglas cylindrical reservoir (40 cm length, 20 mm diameter) with one end of the device connected to the transducer, and the other end with a metal piston. The piston movement during FP was measured with a precision of 6.3 μL. The entire system was filled with physiologic saline. Trauma was induced by the strike of a 1.85-kg pendulum on a Plexiglas cork and the following hydraulic pressure transiently traveling through the device. This wave was impacting upon the dura (the surface area amounted to 113.1 mm^2). The severity of the injury was recorded on a storage oscilloscope (3.8±0.3 atmospheres).

To achieve baseline physiological values, the anaesthesia was reduced to 0.5% isoflurane, and the pigs were allowed to stabilize for 1 h following surgical procedures. In order to monitor the cardiovascular, respiratory and neurophysiological status of each animal, a dataset of required parameters was assessed throughout the experimental performance.

Six hours post injury, animals were sacrificed by intracardial injection of a 30% KCl solution. The brain was quickly removed, the hemispheres were separated sagitally, and the left side (ipsilateral to fluid percussion trauma administration) was immersed in −50°C 2-methylbutane (Carl Roth, Karlsruhe, Germany) for at least 2 minutes. The remaining six animals received all experimental procedures except trauma administration and served as control animals.

In vitro autoradiography

Sagittal whole-brain sections (20 µm) of the ipsilateral hemisphere were cut with a cryostat microtome (MICROM, Walldorf, Germany). Brain slices were mounted onto untreated glass slides [45×75 mm (1 slice); Neolab, Heidelberg, Germany], dried at room temperature, and stored at −28°C for at least 3 days. Slice coordinates were located between 2.0 and 2.6 mm lateral to the midline. In all experiments, two adjacent slices per animal were used for autoradiography.

In vitro autoradiography of [^{3}H]CP-55,940 (Perkin Elmer, Waltham, USA, Lot Number: 626978, specific activity: 144 Ci/mmol) and [^{3}H]SR141716A (Perkin Elmer, Waltham, USA, Lot Number: 3632841, specific activity: 56 Ci/mmol) was performed according to published methods (Herkenham 1991, Herkenham et al. 1991, Glass et al. 1997) with slight modifications. Sections were dried for 15 minutes at room temperature and pre-incubated in buffer (50 mM TRIS-HCl, pH 7.4/21°C), for 15 minutes at room temperature. Slices were then incubated for 60 minutes at room temperature in assay buffer (50 mM TRIS-HCl, 20mM $MgCl_2$, 5 mM EDTA, pH 7.4, 5% bovine serum albumin, Carl Roth, Karlsruhe, Germany) containing the radioligand. The measured ligand concentrations (liquid scintillation counting) were 5 nM for both ([^{3}H] CP-55,940) and ([^{3}H]SR141716A). Non-specific binding was determined on adjacent but lower quality sections in the presence of non-radioactive CP-55,940 (Tocris, Bristol, UK) or SR141716A (Cayman Chemicals, Ann Arbor, USA). After incubation, the slides were washed two times in assay buffer, two times for 30 minutes in washing buffer (50 mM TRIS-HCl, 20 mM $MgCl_2$, 5 mM EDTA, pH 7.4, 1% bovine serum albumin) followed by two times 50 mM TRIS-HCl (pH 7.4/21°C) and dipped in ice-cold ultra-pure water for 10 seconds.

The distribution of TSPO was investigated using a slightly modified method, as published by other authors before (Cumming et al. 2006). Brain slices were dried for 15 minutes, pre-incubated in assay buffer (50 mM TRIS-HCl, pH 7.4/21°C) for 15 minutes and incubated with 0.74 nM [^{3}H]PK11195 (Perkin Elmer, Waltham, USA, Lot Number: 1650101, specific activity: 85.7 Ci/mmol) for 30 min. Slides were washed 2×6 minutes in 50 mM TRIS-HCl, pH 7.4/4°C and dipped twice in ice-cold distilled water.

After washing, all slides were air-dried for 20 minutes, dehydrated over phosphorus pentoxide for at least one day and exposed to BAS-TR2325 imaging plates (Fuji Film, Tokyo, Japan) together with ^{3}H-standards (Micro scales, Amersham, UK) for 4 weeks. Plates were analysed using a Duerr CR-35HD system (Duerr NDT, Bietigheim-Bissinger, Germany). Quantitative analysis of the scan data was performed by computer-assisted microdensitometry (Aida 4.27, Raytest, Straubenhardt, Germany). Irregular regions of interest were drawn over selected areas of the brain. The brain regions of interest were confirmed by Nissl and Gallays staining (Gallyas 1979) on adjacent sections with the help of a pig brain atlas (Felix et al. 1999).

Statistical processing

Data are reported as means ± SD. Two-way analysis of variance (ANOVA), with repeated measures, was used to determine the effects of FP-induced TBI over time and control vs. treatment interaction within each variable of cardiovascular and metabolic response. Subsequently, one-way ANOVA with repeated measures was performed within each group. If normality test failed, one-way ANOVA on ranks, with repeated measures, was used. *Post hoc* comparisons were made with the Holm-Sidak method. Comparisons between groups were made with unpaired *t*-tests using Bonferroni correction for multiple uses, if appropriated. Differences were considered significant when $P<0.05$.

Table I

Effect of fluid percussion induced traumatic brain injury on physiological data including intracranial pressure, brain hemodynamics and oxidative metabolism in newborn piglets. (Sham: *n*=6; Trauma: *n*=7)

	Baseline	Trauma 30 min	Trauma 2 h	Trauma 6 h
Arterial blood pressure (mm Hg)				
Control	68±10	72±8	71±6	64±12
TBI	74±12	76±9	70±12	71±17
Heart rate per min				
Control	244±25	252±23	254±15	253±37
TBI	271±27	282±32	279±28	275±27
Arterial pCO_2 (mm Hg)				
Control	37±3	36±2	40±2	38±3
TBI	35±3	36±1	36±3	35±3
Arterial pH				
Control	7.45±0.05	7.46±0.06	7.42±0.07	7.42±0.12
TBI	7.46±0.02	7.45±0.06	7.45±0.09	7.47±0.03
Arterial pO_2 (mm Hg)				
Control	117±24	121±20	118±18	132±20
TBI	120±24	112±20	118±21	122±29
Intracranial pressure (mm Hg)				
Control	7±3	9±3	9±5	7±5
TBI	8±3	21±9 *$	18±10 *$	11±9
Cerebral perfusion pressure (mm Hg)				
Control	61±10	63±10	61±4	56±9
TBI	66±14	55±12 $	53±17 $	60±16
Cerebral blood flow (mL/100 g/min)				
Control	58±20	52±23	61±23	57±30
TBI	57±19	47±22	48±23	66±28
$CMRO_2$ (mL/100 g/min)				
Control	3.8±1.6	3.3±1.1	3.4±1.3	3.1±1.3
TBI	3.7±1.4	3.4±1.6	3.6±1.4	4.7±2.6

Data are mean ± SD. (TBI) traumatic brain injury. *$ $P<0.05$, *comparison between groups, $ comparison within every group vs. baseline.

RESULTS

Physiological parameters, brain hemodynamics and brain oxidative metabolism

Basic cardiovascular and blood gas, as well as acid-base balance parameters, remained unaltered in control piglets and those receiving FP-TBI. Physiological conditions were consistent with other data obtained from anaesthetized and artificially ventilated newborn piglets (Eisenhauer et al. 1994). During the early period after traumatic injury, FP-TBI elicited a considerable ICP (approx. 50%) increase at a temporary reduced cerebral perfusion pressure (approx. −12%, Table I, $P<0.05$). However, CBF and $CMRO_2$ remained within physiological ranges.

CBR autoradiography with [^{3}H]CP-55,940

Figure 1A shows autoradiographs of the binding of nonselective CBR1/CBR2 receptor ligand [^{3}H]-CP55,940 to adjacent slices of the piglet brain after fluid-percussion induced traumatic brain injury. The receptor densities were quantified in 24 brain regions

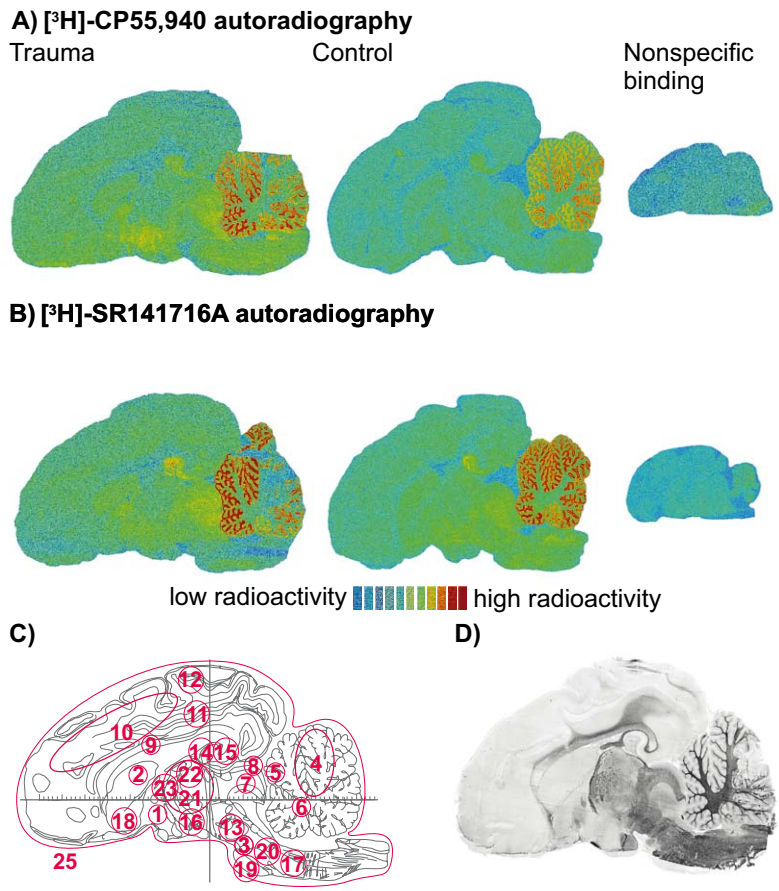

Fig. 1. Autoradiographs of adjacent slices of the piglet brain after fluid-percussion induced traumatic brain injury (A/B, left side) and sham operation (A/B, right side). Images include autoradiographs of [^{3}H]-CP55,940 (A) and [^{3}H]-SR141716A (B) total and nonspecific binding. The receptor densities were quantified in identical brain regions of [^{3}H]CP-55,940 (A) and [^{3}H] SR141716A (B) brain autoradiographs. Additional images show anatomical atlas reference (C) (Felix et al. 1999), with investigated brain regions and a merged image of Cresyl violet/Gallyas stained brain slices after TBI (D) for regional identification (Donat et al. 2010, with permission). Regions of interest are labeled with the following numbers: (1) area hypothalamica anterior; (2) caudate/putamen; (3) central tegmental field; (4) cerebellum; (5) cerebellum, grey matter; (6) cerebellum, white matter; (7) colliculus superior; (8) colliculus superior stratum superficiale; (9) corpus callosum; (10) cortex; (11) cortex, grey matter; (12) cortex, white matter; (13) decussatio pedunculorum cerebellarium superiorum; (14) hippocampus; (15) hippocampus CA1; (16) hypothalamus; (17) medulla; (18) nucleus accumbens; (20) nucleus pontis; (21) nucleus reticularis tegmenti pontis; (22) thalamus; (23) thalamus, dorsalis medialis; (24) thalamus, ventralis posterior; (25) whole brain.

Table II

Cannabinoid receptor density [fmol/mg protein] measured with [^{3}H]CP-55,940; 6 h after fluid-percussion injury in the newborn pig (Sham: n=6; Trauma: n=7)

Region of Interest	Trauma	Sham	% Control	Significance	P-value
Area hypothalamica anterior	137±37.5	72±16.1	190	*	0.002
Caudate/putamen	126±31.0	94±27.7	134		0.079
Central tegmental field	111±30.2	71±19.7	157	*	0.018
Cerebellum	220±40.7	220±63.0	100		0.996
Cerebellum, grey matter	882±263.8	701±205.0	126		0.201
Cerebellum, white matter	92±18.5	81±18.1	114		0.292
Colliculus superior	153±27.8	88±25.4	175	***	0.001
Colliculus superior stratum superficiale	142±33.9	85±19.2	166	**	0.004
Corpus callosum	54±12.3	22±6.1	242	**	0.0001
Cortex	90±10.0	61±15.8	147	**	0.002
Cortex, grey matter	95±12.7	73±13.7	130	*	0.012
Cortex, white matter	53±15.8	44±15.2	119		0.339
Decussatio pedunculorum cerebellarium superiorum	105±29.6	74±10.0	142	*	0.033
Hippocampus	166±35.9	105±28.7	158	**	0.007
Hippocampus CA1	186±37.2	129±37.5	144	*	0.019
Hypothalamus	169±46.8	92±23.6	183	**	0.004
Medulla	107±29.1	81±20.1	132		0.096
Nucleus accumbens	122±30.6	79±21.6	155	*	0.014
Nucleus pontis	73±18.2	60±15.3	121		0.198
Nucleus reticularis tegmenti pontis	109±20.5	75±16.9	145	**	0.008
Thalamus	104±25.7	79±21.5	133		0.077
Thalamus, dorsalis medialis	102±22.0	85±23.3	121		0.190
Thalamus, ventralis posterior	99±19.7	67±19.7	147	*	0.015
Whole brain	122±22.1	89±29.8	138	*	0.040

Data are mean ± SD. Significance tested with the Student's t-test.

and shown in Table II. High CBR densities (>200 fmol/mg protein) were found in the whole cerebellum and the cerebellar grey matter. Moderate binding (100– 200 fmol/mg) was observed in hippocampus, thalamus, midbrain and medulla. Low receptor densities (<100 fmol/mg) are present in the neocortex, cerebellar white matter, corpus callosum and pons.

A marked increase in CBR density was found in 15 brain regions of traumatized animals. This is exemplified by the overall increase of 38% (P<0.05) in whole brains of the injured group compared to control. The strongest increase was found in the corpus callosum (142%, P<0.0001). The neocortex exhibited an increase of 47% (P<0.05), primarily attributed to grey matter (30%, P<0.05). Alterations were also found in other tel-

Table III

Cannabinoid receptor 1 density [fmol/mg protein] measured with [^{3}H]SR141716A; 6 h after fluid-percussion injury in the newborn pig (Sham: n=6; Trauma: n=7)

Region of Interest	Trauma	Sham	% Control	Significance	P-value
Area hypothalamica anterior	283±87.5	251±97.1	113		0.548
Caudate/putamen	357±119.0	316±72.9	113		0.480
Central tegmental field	296±142.9	303±126.5	98		0.935
Cerebellum	747±243.3	886±375.4	84		0.440
Cerebellum, grey matter	2851±1196	2608±891.0	109		0.690
Cerebellum, white matter	213±32.3	236±59.1	90		0.393
Colliculus superior	445±91.1	384±155.0	116		0.394
Colliculus superior stratum superficiale	401±76.0	353±99.1	113		0.351
Corpus callosum	96±12.5	97±27.6	99		0.958
Cortex	202±48.5	179±15.3	113		0.297
Cortex, grey matter	229±87.2	213±82.2	108		0.738
Cortex, white matter	171±64.9	161±67.2	106		0.793
Decussatio pedunculorum cerebellarium superiorum	341±167.1	299±164.6	114		0.653
Hippocampus	545±151.0	476±171.7	114		0.456
Hippocampus CA1	596±173.9	564±269.7	106		0.804
Hypothalamus	416±195.0	371±92.7	112		0.617
Medulla	302±111.6	329±73.6	92		0.621
Nucleus accumbens	252±85.1	239±47.3	106		0.736
Nucleus pontis	259±118.9	251±102.9	103		0.895
Nucleus reticularis tegmenti pontis	310±123.4	291±75.3	107		0.740
Thalamus	293±68.3	255±43.4	115		0.271
Thalamus, dorsalis medialis	292±57.8	252±36.3	116		0.174
Thalamus, ventralis posterior	261±69.8	238±49.4	110		0.520
Whole brain	353±124.9	335±127.4	105		0.805

Data are mean ± SD. Significance tested with the Student's t-test.

encephalic parts of the brain, namely the hippocampus (58%, P<0.01), and cornu ammonis 1 (44%, P<0.05). Within the basal ganglia, the nucleus accumbens exhibited a significant increase (55%, P<0.05), while slightly smaller changes in nucleus caudatus and putamen did not reach the level of significance (34%, P=0.07). Within the diencephalon, the hypothalamus (83%, P<0.01) and the anterior hypothalamic area (90%, P<0.01) showed a strong increase in receptor density. By contrast, within the whole thalamus, rather small alterations were observed (33%, P=0.07). Some parts exhibited significant (ventroposterior part, 46%, P<0.05) others virtually no changes (dorsomedial part). Within the midbrain, the colliculus superior (75%, P<0.01) and especially the stratum superficiale (66%, P≤0.001), decussatio pedunculorum cerebellarium superiorum (41%, P<0.05) and

Table IV

Peripheral-type benzodiazepine receptor density [fmol/mg protein] measured with [^{3}H]PK11195; 6 h after fluid-percussion injury in the newborn pig (Sham: n=6; Trauma: n=7)

Region of Interest	Trauma	Sham	% Control	Significance	P-value
Area hypothalamica anterior	2056±597.2	1517±431.8	136		0.094
Caudateputamen	2162±638.7	2087±642.9	104		0.838
Central tegmental field	1178±330.4	915±237.6	129		0.134
Cerebellum	609±146.2	536±153.5	113		0.403
Cerebellum, grey matter	1194±264.6	1066±320.2	112		0.446
Cerebellum, white matter	475±138.0	525±160.4	90		0.552
Colliculus superior	1583±566.2	1652±398.4	96		0.809
Colliculus superior stratum superficiale	2082±655.5	2238±462.0	93		0.637
Corpus callosum	1143±327.5	905±208.2	126		0.154
Cortex	1231±259.6	1173±341.4	105		0.737
Cortex, grey matter	1839±408.9	2062±344.7	89		0.316
Cortex, white matter	941±255.4	948±246.2	99		0.963
Decussatio pedunculorum cerebellarium superiorum	1178±297.5	1030±287.9	114		0.383
Hippocampus	1138±344.6	1066±259.9	107		0.684
Hippocampus CA1	1174±345.3	1038±254.7	113		0.445
Hypothalamus	1618±463.9	1205±230.1	134		0.074
Medulla	654±150.4	730±182.8	90		0.426
Nucleus accumbens	1764±287.8	1602±346.0	110		0.377
Nucleus pontis	1210±264.8	1093±317.2	111		0.483
Nucleus reticularis tegmenti pontis	1081±243.7	989±264.4	109		0.528
Thalamus	1859±489.0	1896±522.9	98		0.896
Thalamus, dorsalis medialis	2062±561.1	2050±551.9	101		0.971
Thalamus, ventralis posterior	1884±519.7	1755±432.0	107		0.639
Whole brain	1314±307.1	1321±322.4	99		0.970

Data are mean ± SD. Significance tested with the Student's t-test.

the central tegmental field (57%, P<0.05) showed significantly increased receptor densities. Within the pons, the nucleus reticularis tegmenti pontis (45%, P<0.01) was found to exhibit increased binding after injury, while the nuclei pontis remained largely unchanged. No changes were observed in the brainstem, which also applies for the whole cerebellum, cerebellar grey and white matter.

CB1R autoradiography with [^{3}H]SR141716A

For autoradiography with CBR1-selective radioligand [^{3}H]SR141716A, the receptor densities in discrete brain regions of control animals correlated well with those found in [^{3}H]CP-55,940 autoradiography (r=0.99, Table II, III), however the absolute values were about twofold higher, probably caused by differences bind-

ing mechanism (agonist vs. antagonist binding) of the two different radioligands applied.

Comparison of CB1R densities by [^{3}H]SR141716A autoradiography of traumatized and control animals showed no statistically significant differences between both groups.

Autoradiography of TSPO with [^{3}H]PK11195

Autoradiography of TSPO, a biomarker for gliosis/brain injury (Chen and Guilarte 2008, Karlstetter et al. 2014) with 0.7 nM [^{3}H]PK11195 revealed densities in sham-operated animals between 525 fmol/mg (cerebellar white matter) and 2238 fmol/mg in stratum superficiale of the superior colliculi (Table IV). These values are slightly higher as previously found in adult pigs (Cumming et al. 2006), although their regional distribution was similar. FP-TBI did not significantly alter TSPO density, although increases of up to ~35% in binding were found in various brain regions.

DISCUSSION

This is the first study demonstrating significant increases in cannabinoid receptor density after traumatic brain injury. It shows that binding of the non-selective agonist [^{3}H]CP-55,940, a ligand with nearly equal affinity to CB1R and CB2R (Felder et al. 1992), is significantly increased in most of the investigated brain regions of newborn piglets at 6 hours after fluid-percussion induced TBI. Comparative autoradiography with the antagonist [^{3}H]SR141716A, a selective CB1R ligand, in the employed low nanomolar range (Rinaldi-Carmona et al. 1994, White and Hiley 1998, Pertwee 2000), did not revealed significant changes after TBI. Therefore, we conclude that the increase in [^{3}H]CP-55,940 binding mainly reflects an TBI-related increase of CB2R density in the brain. [^{3}H]CP-55,940 is regarded to be selective towards CBR, although it also binds to the GPR55 receptor with 25-fold lower binding potency compared to CB1R (Ryberg et al. 2007). The radioligand shows comparable binding patterns and receptor densities among different species (Herkenham et al. 1990, Westlake et al. 1994), although interspecies regional differences exist (Glass et al. 1997, Harkany et al. 2005, McPartland et al. 2007). For both [^{3}H]CP-55,940 and [^{3}H]SR141716A, a high binding is observed in the basal ganglia, hippocampus (dentate gyrus) and in the molecular layer of the cerebellum. Low binding is present in the thalamus and brainstem. This distribution pattern was also found in this study, therefore being in line with previously reported data, although the authors are not aware of any papers on CBR autoradiography in the pig brain.

In our study, the newborn piglets were subjected to a diffuse FP-TBI with considerable cardiovascular, metabolic, and neurophysiological monitoring throughout the experiment, as reported before (Donat et al. 2010a). For this animal model of paediatric TBI, we have shown that the systemic cardiovascular and ventilator parameters remained within physiological ranges and cerebral perfusion pressure and brain oxygen delivery/consumption did not show critical disturbances (Donat et al. 2010a). Thus we assume that confounding neuropathological processes connected to the eCB system, such as ischemia (Capettini et al. 2012) and hypoxia (Pazos et al. 2013), are of little impact.

The observed regional differences in CBR binding after TBI may be attributed to (bio)mechanical stress and distance from injury. Different regions of the brain are exposed to varying levels of mechanical stress during TBI, which is an inherent part of this model and has been analysed *in silico* (Cloots et al. 2008, Bayly et al. 2012). Furthermore, the biomechanical properties of the immature brain differ from those of the adult brain (LaPlaca et al. 2007, Finnie 2012), especially the viscoelastic response of brain tissue is a dynamic phenomenon (Feng et al. 2013). Furthermore, no significant changes in CBR density were observed in cerebellum and brainstem, which are located at the greatest distance from the impact site. Therefore, the question remain, whether the suggested CB2R upregulation is attributed to a direct biomechanical impact and/or secondary injury effects related to differences in bio(mechanical) stress. Such an effect has been already discussed in recent studies, reporting on region-specific alterations in the densities of cholinergic receptors and transporters, with patterns comparable to the changes in CBR densities observed in this study (Donat et al. 2010a,b, Hoffmeister et al. 2011). Interestingly, the strongest increases of CBR density in our study was detected in corpus callosum (+142%), known as highly vulnerable to diffuse/traumatic axonal injury both in experimental models (Hicks et al. 1997, Saatman et al. 1998, Graham et al. 2000) and patients (Leclercq et al. 2001, Gorrie et al. 2002, Babikian et al. 2010). These increases could be caused by an impaired

axonal transport, which was found for amyloid precursor protein after TBI (Stone et al. 2004) and CBR after ligation of the sciatic nerve (Hohmann and Herkenham 1999).

Besides biomechanical and axonal injury, an inflammation-related increase in CBR2 expression needs to be considered. Inflammatory changes are described in many neurodegenerative diseases (Ashton and Glass 2007), including TBI (Finnie 2013), and CBR antagonist application prevents the neuroprotection by minocycline in a mouse model of head injury (Lopez-Rodriguez et al. 2013). In contrast, several other studies using eCB or CB1R/CB2R agonists showed the neuroprotective efficacy of those compounds in both experimental and human TBI (Panikashvili et al. 2001, Mauler et al. 2003, Cohen-Yeshurun et al. 2011, Firsching et al. 2012, Horvath et al. 2012). In a mouse model, the strongest neurodegenerative and behavioral effects were found at 24 h post-TBI and application of the CB2R selective agonist O-1966 ameliorated these effects (Elliott et al. 2011, Amenta et al. 2012). The latter corresponds with the time frames of microglial activation in other models of acute brain injuries, with microglial activation and proliferation starting immediately after injury but reaching its maximum not until 1 day post injury (Jin et al. 2010). Such delay in microglial activation and proliferation could be the reason for non-significant TBI-related changes in TSPO densities, an important target in head trauma (Papadopoulos and Lecanu 2009), in our model at 6 h post injury, although the slightly increased binding of [^{3}H]PK11195 in 16 out of 24 investigated brain regions may indicate early proliferation of microglial cells. Noteworthy is a region-specific correlation between the TBI-related increase of [^{3}H]PK11195 and [^{3}H]CP-55,940, with maximum effects observed in hypothalamic areas, central tegmental field, and corpus callosum. It may be speculated that these similarities point to a common cellular origin and are caused by the secondary pathophysiological changes after TBI. Activated microglia could be this common cellular origin, because they are known to exert both degenerative and reparative actions in the injured/recovering brain after TBI (Helmy et al. 2011). Activated microglial cells show both an upregulation of CB2R (Maresz et al. 2005) and express TSPO (Cosenza-Nashat et al. 2009, Karlstetter et al. 2014), which is supporting this assumption.

CONCLUSION

In this study, we could show an increase in the density of CBR already at 6 hours after experimental TBI in newborn piglets, a model with high relevance for paediatric TBI. Irrespectively of the sources and causes of the observed effect, the (endo)cannabinoid system is regarded as highly relevant in TBI (Shohami et al. 2011), both in terms of pathological mechanisms and for the development of neuroprotective therapies. In preclinical research of TBI, the CB2R therefore may be an interesting target for molecular *in vivo* imaging, either as early marker of brain injury or for validation of CB2R-targeting drugs. Altogether, the role of CBR and especially CB2R along with the exact time course of changes after TBI remains to be elucidated.

ACKNOWLEDGMENTS

The authors thank Mrs. R.M. Zimmer for their skilful technical assistance.

REFERENCES

Amenta PS, Jallo JI, Tuma RF, Elliott MB (2012) A cannabinoid type 2 receptor agonist attenuates blood-brain barrier damage and neurodegeneration in a murine model of traumatic brain injury. J Neurosci Res 90: 2293–2305.

Anderson V, Catroppa C, Morse S, Haritou F, Rosenfeld J (2005) Functional plasticity or vulnerability after early brain injury? Pediatrics 116: 1374–1382.

Anderson V, Catroppa C, Morse S, Haritou F, Rosenfeld JV (2009) Intellectual outcome from preschool traumatic brain injury: a 5-year prospective, longitudinal study. Pediatrics 124: e1064–1071.

Ashton JC, Glass M (2007) The cannabinoid CB2 receptor as a target for inflammation-dependent neurodegeneration. Curr Neuropharmacol 5: 73–80.

Babikian T, Marion SD, Copeland S, Alger JR, O'Neill J, Cazalis F, Mink R, Giza CC, Vu JA, Hilleary SM, Kernan CL, Newman N, Asarnow RF (2010) Metabolic levels in the corpus callosum and their structural and behavioral correlates after moderate to severe pediatric TBI. J Neurotrauma 27: 473–481.

Bahr BA, Karanian DA, Makanji SS, Makriyannis A (2006) Targeting the endocannabinoid system in treating brain disorders. Expert Opin Investig Drugs 15: 351–365.

Barlow KM, Thomson E, Johnson D, Minns RA (2005) Late neurologic and cognitive sequelae of inflicted traumatic brain injury in infancy. Pediatrics 116: e174–185.

Bauer R, Fritz H (2004) Pathophysiology of traumatic injury in the developing brain: an introduction and short update. Exp Toxicol Pathol 56: 65–73.

Bayir H, Kochanek PM, Kagan VE (2006) Oxidative stress in immature brain after traumatic brain injury. Dev Neurosci 28: 420–431.

Bayly PV, Clayton EH, Genin GM (2012) Quantitative imaging methods for the development and validation of brain biomechanics models. Annu Rev Biomed Eng 14: 369–396.

Capettini LS, Savergnini SQ, da Silva RF, Stergiopulos N, Santos RA, Mach F, Montecucco F (2012) Update on the role of cannabinoid receptors after ischemic stroke. Mediators Inflamm 2012: 824093.

Cederberg D, Siesjo P (2010) What has inflammation to do with traumatic brain injury? Childs Nerv Syst 26: 221–226.

Chen MK, Guilarte TR (2008) Translocator protein 18 kDa (TSPO): molecular sensor of brain injury and repair. Pharmacol Ther 118: 1–17.

Cloots RJ, Gervaise HM, van Dommelen JA, Geers MG (2008) Biomechanics of traumatic brain injury: influences of the morphologic heterogeneities of the cerebral cortex. Ann Biomed Eng 36: 1203–1215.

Cohen-Yeshurun A, Trembovler V, Alexandrovich A, Ryberg E, Greasley PJ, Mechoulam R, Shohami E, Leker RR (2011) N-arachidonoyl-L-serine is neuroprotective after traumatic brain injury by reducing apoptosis. J Cereb Blood Flow Metab 31: 1768–1777.

Cosenza-Nashat M, Zhao ML, Suh HS, Morgan J, Natividad R, Morgello S, Lee SC (2009) Expression of the translocator protein of 18 kDa by microglia, macrophages and astrocytes based on immunohistochemical localization in abnormal human brain. Neuropathol Appl Neurobiol 35: 306–328.

Coyle MG, Oh W, Stonestreet BS (1993) Effects of indomethacin on brain blood flow and cerebral metabolism in hypoxic newborn piglets. Am J Physiol 264: H141–149.

Cumming P, Pedersen MD, Minuzzi L, Mezzomo K, Danielsen EH, Iversen P, Aagaard D, Keiding S, Munk OL, Finsen B (2006) Distribution of PK11195 binding sites in porcine brain studied by autoradiography in vitro and by positron emission tomography. Synapse 59: 418–426.

Donat CK, Walter B, Deuther-Conrad W, Wenzel B, Nieber K, Bauer R, Brust P (2010a) Alterations of cholinergic receptors and the vesicular acetylcholine transporter after lateral fluid percussion injury in newborn piglets. Neuropathol Appl Neurobiol 36: 225–236.

Donat CK, Walter B, Kayser T, Deuther-Conrad W, Schliebs R, Nieber K, Bauer R, Hartig W, Brust P (2010b) Effects of lateral fluid percussion injury on cholinergic markers in the newborn piglet brain. Int J Dev Neurosci 28: 31–38.

Eisenhauer CL, Matsuda LS, Uyehara CF (1994) Normal physiologic values of neonatal pigs and the effects of isoflurane and pentobarbital anesthesia. Lab Anim Sci 44: 245–252.

Elliott MB, Tuma RF, Amenta PS, Barbe MF, Jallo JI (2011) Acute effects of a selective cannabinoid-2 receptor agonist on neuroinflammation in a model of traumatic brain injury. J Neurotrauma 28: 973–981.

Felder CC, Veluz JS, Williams HL, Briley EM, Matsuda LA (1992) Cannabinoid agonists stimulate both receptor- and non-receptor-mediated signal transduction pathways in cells transfected with and expressing cannabinoid receptor clones. Mol Pharmacol 42: 838–845.

Felix B, Leger ME, Albe-Fessard D, Marcilloux JC, RampinO, Laplace JP (1999) Stereotaxic atlas of the pig brain. Brain Res Bull 49: 1–137.

Feng Y, Clayton EH, Chang Y, Okamoto RJ, Bayly PV (2013) Viscoelastic properties of the ferret brain measured in vivo at multiple frequencies by magnetic resonance elastography. J Biomech 46: 863–870.

Finnie JW (2012) Comparative approach to understanding traumatic injury in the immature, postnatal brain of domestic animals. Aust Vet J 90: 301–307.

Finnie JW (2013) Neuroinflammation: beneficial and detrimental effects after traumatic brain injury. Inflammopharmacology 21: 309–320.

Firsching R, Piek J, Skalej M, Rohde V, Schmidt U, Striggow F, Group KNS (2012) Early survival of comatose patients after severe traumatic brain injury with the dual cannabinoid CB1/CB2 receptor agonist KN38-7271: a randomized, double-blind, placebo-controlled phase II trial. J Neurol Surg A Cent Eur Neurosurg 73: 204–216.

Gallyas F (1979) Silver staining of myelin by means of physical development. Neurol Res 1: 203–209.

Giza CC, Mink RB, Madikians A (2007) Pediatric traumatic brain injury: not just little adults. Curr Opin Crit Care 13: 143–152.

Glass M, Dragunow M, Faull RL (1997) Cannabinoid receptors in the human brain: a detailed anatomical and quantitative autoradiographic study in the fetal, neonatal and adult human brain. Neuroscience 77: 299–318.

Gorrie C, Oakes S, Duflou J, Blumbergs P, Waite PM (2002) Axonal injury in children after motor vehicle crashes: extent, distribution, and size of axonal swellings using beta-APP immunohistochemistry. J Neurotrauma 19: 1171–1182.

Graham DI, Raghupathi R, Saatman KE, Meaney D, McIntosh TK (2000) Tissue tears in the white matter after lateral fluid percussion brain injury in the rat: relevance to human brain injury. Acta Neuropathol 99: 117–124.

Harkany T, Dobszay MB, Cayetanot F, Hartig W, Siegemund T, Aujard F, Mackie K (2005) Redistribution of CB1 cannabinoid receptors during evolution of cholinergic basal forebrain territories and their cortical projection areas: a comparison between the gray mouse lemur (Microcebus murinus, primates) and rat. Neuroscience 135: 595–609.

Helmy A, De Simoni MG, Guilfoyle MR, Carpenter KL, Hutchinson PJ (2011) Cytokines and innate inflammation in the pathogenesis of human traumatic brain injury. Prog Neurobiol 95: 352–372.

Herkenham M, Lynn AB, Little MD, Johnson MR, Melvin LS, de Costa BR, Rice KC (1990) Cannabinoid receptor localization in brain. Proc Natl Acad Sci U S A 87: 1932–1936.

Herkenham M (1991) Characterization and localization of cannabinoid receptors in brain: an in vitro technique using slide-mounted tissue sections. NIDA Res Monogr 112: 129–145.

Herkenham M, Lynn AB, Johnson MR, Melvin LS, de Costa BR, Rice KC (1991) Characterization and localization of cannabinoid receptors in rat brain: a quantitative in vitro autoradiographic study. J Neurosci 11: 563–583.

Hicks RR, Baldwin SA, Scheff SW (1997) Serum extravasation and cytoskeletal alterations following traumatic brain injury in rats. Comparison of lateral fluid percussion and cortical impact models. Mol Chem Neuropathol 32: 1–16.

Hoffmeister PG, Donat CK, Schuhmann MU, Voigt C, Walter B, Nieber K, Meixensberger J, Bauer R, Brust P (2011) Traumatic brain injury elicits similar alterations in alpha7 nicotinic receptor density in two different experimental models. Neuromolecular Med 13: 44–53.

Hohmann AG, Herkenham M (1999) Cannabinoid receptors undergo axonal flow in sensory nerves. Neuroscience 92: 1171–1175.

Horvath B, Magid L, Mukhopadhyay P, Batkai S, Rajesh M, Park O, Tanchian G, Gao RY, Goodfellow CE, Glass M, Mechoulam R, Pacher P (2012) A new cannabinoid CB2 receptor agonist HU-910 attenuates oxidative stress, inflammation and cell death associated with hepatic ischaemia/reperfusion injury. Br J Pharmacol 165: 2462–2478.

Jankowitz BT, Adelson PD (2006) Pediatric traumatic brain injury: past, present and future. Dev Neurosci 28: 264–275.

Jin R, Yang G, Li G (2010) Inflammatory mechanisms in ischemic stroke: role of inflammatory cells. J Leukoc Biol 87: 779–789.

Karlstetter M, Nothdurfter C, Aslanidis A, Moeller K, Horn F, Scholz R, Neumann H, Weber BH, Rupprecht R, Langmann T (2014) Translocator protein (18 kDa) (TSPO) is expressed in reactive retinal microglia and modulates microglial inflammation and phagocytosis. J Neuroinflammation 11: 3.

Keenan HT, Bratton SL (2006) Epidemiology and outcomes of pediatric traumatic brain injury. Dev Neurosci 28: 256–263.

Kennard MA (1942) Cortical reorganization of motor function: studies on a series of mon-keys of various ages from infancy to maturity. Arch Neurol Psychiatry 48: 227–240.

Kochanek PM (2006) Pediatric traumatic brain injury: quo vadis? Developmental neuroscience 28: 244–255.

LaPlaca MC, Simon CM, Prado GR, Cullen DK (2007) CNS injury biomechanics and experimental models. Prog Brain Res 161: 13–26.

Leclercq PD, McKenzie JE, Graham DI, Gentleman SM (2001) Axonal injury is accentuated in the caudal corpus callosum of head-injured patients. J Neurotrauma 18: 1–9.

Li L, Liu J (2013) The effect of pediatric traumatic brain injury on behavioral outcomes: a systematic review. Dev Med Child Neurol 55: 37–45.

Li LM, Menon DK, Janowitz T (2014) Cross-sectional analysis of data from the U.S. clinical trials database reveals poor translational clinical trial effort for traumatic brain injury, compared with stroke. PLoS One 9: e84336.

Lopez-Rodriguez AB, Siopi E, Finn DP, Marchand-Leroux C, Garcia-Segura LM, Jafarian-Tehrani M, Viveros MP (2013) CB1 and CB2 cannabinoid receptor antagonists prevent minocycline-induced neuroprotection following traumatic brain injury in mice. Cereb Cortex [Epub ahead of print].

Luo P, Fei F, Zhang L, Qu Y, Fei Z (2011) The role of glutamate receptors in traumatic brain injury: Implications for postsynaptic density in pathophysiology. Brain Res Bull 85: 313–320.

Makowski EL, Meschia G, Droegemueller W, Battaglia FC (1968) Measurement of umbilical arterial blood flow to the sheep placenta and fetus in utero. Distribution to cotyledons and the intercotyledonary chorion. Circ Res 23: 623–631.

Maresz K, Carrier EJ, Ponomarev ED, Hillard CJ, Dittel BN (2005) Modulation of the cannabinoid CB2 receptor in microglial cells in response to inflammatory stimuli. J Neurochem 95: 437–445.

Masel BE, DeWitt DS (2010) Traumatic brain injury: a disease process, not an event. J Neurotrauma 27: 1529–1540.

Mauler F, Hinz V, Augstein KH, Fassbender M, Horvath E (2003) Neuroprotective and brain edema-reducing efficacy of the novel cannabinoid receptor agonist BAY 38-7271. Brain Res 989: 99–111.

McConeghy KW, Hatton J, Hughes L, Cook AM (2012) A review of neuroprotection pharmacology and therapies in patients with acute traumatic brain injury. CNS Drugs 26: 613–636.

McPartland JM, Glass M, Pertwee RG (2007) Meta-analysis of cannabinoid ligand binding affinity and receptor distribution: interspecies differences. Br J Pharmacol 152: 583–593.

Miller LK, Devi LA (2011) The highs and lows of cannabinoid receptor expression in disease: mechanisms and their therapeutic implications. Pharmacol Rev 63: 461–470.

Panikashvili D, Simeonidou C, Ben-Shabat S, Hanus L, Breuer A, Mechoulam R, Shohami E (2001) An endogenous cannabinoid (2-AG) is neuroprotective after brain injury. Nature 413: 527–531.

Papadopoulos V, Lecanu L (2009) Translocator protein (18 kDa) TSPO: an emerging therapeutic target in neurotrauma. Exp Neurol 219: 53–57.

Pazos MR, Mohammed N, Lafuente H, Santos M, Martinez-Pinilla E, Moreno E, Valdizan E, Romero J, Pazos A, Franco R, Hillard CJ, Alvarez FJ, Martinez-Orgado J (2013) Mechanisms of cannabidiol neuroprotection in hypoxic-ischemic newborn pigs: role of 5HT(1A) and CB2 receptors. Neuropharmacology 71: 282–291.

Pertwee RG (2000) Cannabinoid receptor ligands: clinical and neuropharmacological considerations, relevant to future drug discovery and development. Expert Opin Investig Drugs 9: 1553–1571.

Rinaldi-Carmona M, Barth F, Heaulme M, Shire D, Calandra B, Congy C, Martinez S, Maruani J, Neliat G, Caput D, et al. (1994) SR141716A, a potent and selective antagonist of the brain cannabinoid receptor. FEBS Lett 350: 240–244.

Ryberg E, Larsson N, Sjogren S, Hjorth S, Hermansson NO, Leonova J, Elebring T, Nilsson K, Drmota T, Greasley PJ (2007) The orphan receptor GPR55 is a novel cannabinoid receptor. Br J Pharmacol 152: 1092–1101.

Saatman KE, Graham DI, McIntosh TK (1998) The neuronal cytoskeleton is at risk after mild and moderate brain injury. J Neurotrauma 15: 1047–1058.

Sarne Y, Asaf F, Fishbein M, Gafni M, Keren O (2011) The dual neuroprotective-neurotoxic profile of cannabinoid drugs. Br J Pharmacol 163: 1391–1401.

Shohami E, Cohen-Yeshurun A, Magid L, Algali M, Mechoulam R (2011) Endocannabinoids and traumatic brain injury. Br J Pharmacol 163: 1402–1410.

Stone JR, Okonkwo DO, Dialo AO, Rubin DG, Mutlu LK, Povlishock JT, Helm GA (2004) Impaired axonal transport and altered axolemmal permeability occur in distinct populations of damaged axons following traumatic brain injury. Exp Neurol 190: 59–69.

Sullivan HG, Martinez J, Becker DP, Miller JD, Griffith R, Wist AO (1976) Fluid-percussion model of mechanical brain injury in the cat. J Neurosurg 45: 521–534.

Taylor HG, Swartwout MD, Yeates KO, Walz NC, Stancin T, Wade SL (2008) Traumatic brain injury in young children: postacute effects on cognitive and school readiness skills. J Int Neuropsychol Soc 14: 734–745.

Tolias CM, Bullock MR (2004) Critical appraisal of neuroprotection trials in head injury: what have we learned? NeuroRx 1: 71–79.

Walter B, Bauer R, Gaser E, Zwiener U (1997) Validation of the multiple colored microsphere technique for regional blood flow measurements in newborn piglets. Basic Res Cardiol 92: 191–200.

Weber JT (2004) Calcium homeostasis following traumatic neuronal injury. Curr Neurovasc Res 1: 151–171.

Westlake TM, Howlett AC, Bonner TI, Matsuda LA, Herkenham M (1994) Cannabinoid receptor binding and messenger RNA expression in human brain: an in vitro receptor autoradiography and in situ hybridization histochemistry study of normal aged and Alzheimer's brains. Neuroscience 63: 637–652.

White R, Hiley CR (1998) The actions of the cannabinoid receptor antagonist, SR 141716A, in the rat isolated mesenteric artery. Br J Pharmacol 125: 689–696.